Quantifying the respective roles of aerosols and clouds in the strong brightening since the early 2000s over the Iberian Peninsula

D. Mateos[1*], A. Sanchez-Lorenzo[2,3], M. Antón[4,5], V.E. Cachorro[1], J. Calbó[2], M.J. Costa[5], B. Torres[1], M. Wild[6]

[1]Grupo de Óptica Atmosférica, University of Valladolid, Valladolid, Spain, *e-mail: mateos@goa.uva.es

[2]Group of Environmental Physics, University of Girona, Girona, Spain

[3]Instituto Pirenaico de Ecología, Consejo Superior de Investigaciones Científicas (IPE-CSIC), Zaragoza, Spain

[4]Department of Physics, University of Extremadura, Badajoz, Spain

[5]Évora Geophysics Centre and Dep. Physics, University of Évora, Évora, Portugal

[6]Institute for Atmospheric and Climate Science, ETH Zurich, Zurich, Switzerland

Abstract

The contribution of clouds and aerosols to the decadal variations of downward surface shortwave radiation (SSR) is a current controversial topic. This study proposes a method, which is based on surface-based SSR measurements, aerosol observations, and radiative transfer simulations (in cloud-free and cloud- and aerosol-free scenarios), to evaluate cloud-aerosol (CARE), cloud (CRE), and aerosol (ARE) radiative effects. This method is applied to quantify the role played by, separately, clouds and aerosols on the intense brightening of the SSR observed in the Iberian Peninsula. Clouds and Earth's Radiation Energy Budget System (CERES) and surface-based data exhibit an increase in SSR between 2003 and 2012, exceeding +10 Wm^{-2} over this period for some areas of the peninsula. The calculations are performed for three surface-based sites: Barcelona and Valladolid (Spain), and Évora (Portugal). Ranges in monthly values of CARE, CRE, and ARE are (-80, -20), (-60, -20), and (-30, 0), respectively (in Wm^{-2}). The average trends for the analyzed period of CARE, CRE, and ARE are +7, +5, and +2 Wm^{-2} per decade, respectively. Overall, three-fourths of the SSR trend is explained by clouds, while the other one-fourth is related to aerosol changes. The SSR trends explained by the clouds and aerosol radiative effects are in line with the observed reductions in total cloud cover and aerosol load (both at the surface and in the whole atmospheric column). Furthermore, the CRE values are compared against CERES data showing good agreement between both data series, although some discrepancies are observed in their trends.

Keywords: downward shortwave radiation trend; brightening period; cloud and aerosol radiative effects; total cloud cover and aerosol load

Key Points:

1) A strong brightening is observed between 2003 and 2012 in the Iberian Peninsula

2) Solar radiation change is explained 75% by clouds and 25% by aerosols

3) Cloud radiative effect from CERES and surface-based data are in good agreement

1. Introduction

Trends of downward surface shortwave radiation (SSR) have received much attention due to their role in climate change. Variations of the SSR levels may cause a relevant effect on the planetary radiative budget [*Trenberth et al.*, 2009; *Stephens et al.*, 2012; *Wild et al.*, 2013], hydrological cycle [e.g., *Niemeier et al.*, 2013; *Wang and Yang*, 2014], and carbon cycle [e.g., *Ramanathan and Carmichael*, 2008].

Regarding trends in SSR, two different periods have been distinguished in many regions worldwide: a decreasing trend in SSR from the early 1960s to the 1980s, and an increasing trend beyond the late 1980s. The first period is known as the dimming period [*Stanhill and Cohen*, 2001], while the second one is the brightening period (BP) [*Wild et al.*, 2005]. All these decadal variations in SSR were mainly attributed to variations in clouds and aerosols and the interactions between them [*Wild*, 2009]. Changes in the concentration of various atmospheric gases such as ozone and water vapor play a negligible role on the significant long-term variations detected in the incoming SSR at the surface [e.g., *Kvalevag and Myhre*, 2007; *Antón and Mateos*, 2013; *Mateos et al.*, 2013]. Nevertheless, the relative contribution of clouds and aerosols to the temporal changes in SSR is not clear yet [e.g., *Norris and Wild*, 2009; *Chiacchio and Vitolo*, 2012; *Kawamoto and Hayasaka*, 2012]. On the one hand, the discussion of aerosol radiative effects is usually restricted to cloud-free conditions. For instance, *Ruckstuhl et al.* [2008] have found for Northern Germany and Switzerland a strong decline in aerosol load of about 60% since the 1980s, which is responsible for the BP under cloud-free skies. Hence, the direct aerosol effect is suggested as the dominant one on modulating the radiative budget [*Philipona et al.*, 2009]. Equally, *Kudo et al.* [2012] attributed the BP over Japan to changes in aerosol properties, particularly the single scattering albedo, since clouds exhibit no significant trend for the same period. With respect to aerosol indirect effect, *Ruckstuhl et al.* [2010] found a small contribution (five times smaller than the direct effect) to the BP over Europe. All of these studies agree in pointing out aerosols as the main factor modulating the BP during the last decades.

Nevertheless, the long-term contribution of the cloud radiative effect is a matter of controversy. Some studies state that clouds seem to contribute in a lesser extent to the SSR changes than aerosols [e.g., *Norris and Wild*, 2007; *Ruckstuhl et al.*, 2008; *Ruckstuhl and Norris*, 2009]. However, other studies indicate that decrease in cloud cover as well as changes in the cloud types and cloud optical properties are the main responsible for the BP. For instance, *Hatzianastassiou et al.* [2005] found that low-level clouds can explain up to 70% of the BP observed between 1984 and 2000 on a detailed global-scale analysis. *Stjern et al.* [2009] analyzed the relationship between SSR records and cloud cover and aerosol information at 11 stations in northwestern Europe and the European Arctic. Their results showed that SSR changes can be mainly explained by variations in cloud cover in most cases. *Yang et al.* [2011] stated that cloud and aerosol effects on BP over the Tibetan Plateau are comparable. In addition, *Liley* [2009] suggested that brightening in New Zealand was also due to changes in cloudiness. Similarly, *Long et al.* [2009] and *Augustine and Dutton* [2013] concluded that changes in aerosols alone cannot explain the observed SSR changes in the USA since 1996. Therefore, the contribution of the atmospheric factors responsible for the increasing trend in SSR needs to be more thoroughly investigated.

In a previous study, *Mateos et al.* [2013] described a methodology to obtain the radiative effects for the cloud-aerosol system as a whole. The current study goes further in the characterization of the radiative effects caused separately by each factor. The method proposed in this paper to discriminate between cloud and aerosol radiative effects is based on measurements of SSR and aerosol properties, and radiative transfer simulations. Therefore, it can be applied at a large number of stations worldwide. To our knowledge, this study is the first effort in the use of surface-based data (both SSR and columnar aerosols observations) in the separate retrieval of the long-term radiative effects related to clouds and aerosols. As discussed in the present study, an intense and recent BP was observed for the Iberian Peninsula (Southwestern Europe) starting in the early 2000s [e.g., *Bilbao et al.*, 2011; *Sanchez-Lorenzo et al.*, 2013a]. Taking advantage of this phenomenon, the proposed method is applied to obtain separate cloud and aerosol radiative effects, and their temporal variations, for this region and time period.

2. Database

Spanish SSR measurements were provided by the Spanish Meteorological Agency (AEMET). The same collection of 13 data series extensively described by *Sanchez-Lorenzo et al.* [2013a] is used in this study to document brightening over the Iberian Peninsula. Details about calibration, quality control, and homogenization were described by these authors. SSR measurements (305-2800 nm) have been performed by using Kipp & Zonen pyranometers with an expected daily relative uncertainty <5% [e.g., *Bilbao et al.*, 2011]. In addition, the site Barcelona is also used because it has coincident aerosol data. The same procedures are applied to this latter time series. The Portuguese station used in this study is located in the city of Évora and maintained by the University of Évora. At this station, an Eppley black and white pyranometer records SSR. This time series was validated against a nearby site (Mitra, with a Kipp&Zonen albedometer) and compared very well (not shown).

Monthly mean of aerosol properties are obtained from the Aerosol Robotic Network (AERONET). Level 2.0 data are downloaded in order to obtain reliable aerosol information of aerosol optical depth (AOD) and Ångström coefficient α [e.g., *Toledano et al.*, 2007]. The advantage of level 2.0 (quality-assured) with respect to other levels is that the data are calibrated before and after a measurement period (usually about one year), cloud-screened, and manually inspected to ensure high quality aerosol data. According to *Holben et al.* [1998], the estimated uncertainty is 0.01–0.02 for the aerosol optical depth. Monthly gaps of aerosol data are filled with the corresponding monthly climatological mean for the whole analyzed period. The number of filled gaps are 3, 17, and 19 for the sites Valladolid, Barcelona and Évora, respectively. The data gaps in the Barcelona and Evora time series all occurred in the first year of each time series and in 2006. The filling of these gaps (<15% of the entire dataset) is necessary to better reproduce the temporal trends of the aerosol effects [e.g., *Bennouna et al.*, 2014]. Values of AOD at 440 and 1020 nm, and α coefficient are used as input in the simulations described in the next section.

Locations with both aerosol and SSR measurements are required in this study for the longest possible period. Only three sites in the Iberian Peninsula offer high-quality, long-term, and collocated SSR and aerosol data: Barcelona, Évora, and Valladolid (which uses aerosol information from 40 km away at Palencia). All required variables are available since 2003 for Valladolid and Évora, and since 2004 for Barcelona. Table 1 shows the geographical information of the three stations. The distance between aerosol and radiation sites seems not to be a disadvantage since the columnar aerosol observations are representative for the background aerosols over each area. For instance, Palencia aerosol data are representative for the "Castilla and León" region, which is not affected by high pollution conditions; hence, they are adequate to characterize the aerosol information of the site Valladolid.

The Clouds and the Earth's Radiant Energy System (CERES) EBAF (Energy Balanced And Filled)-Surface data set (Ed2.7) [*Kato et al.*, 2013] is also used in this study. This data set provides a wide spatial and long temporal coverage of radiative products that can be compared with the surface-based results presented in this study. These data were obtained from the NASA Langley Research Center (http://ceres.larc.nasa.gov/). CERES is a three-channel radiometer measuring solar radiation (0.3-5 μm), emitted terrestrial radiation (8-12 μm), and total radiation (0.3->100 μm) with a spatial resolution of 20 km at nadir. The EBAF-Surface product provides computed monthly mean surface radiative fluxes [*Kato et al.*, 2013]. Two products from the CERES EBAF-Surface database are used: downward surface shortwave radiation (SSR_{CERES}), and surface shortwave cloud radiative effect (CRE_{CERES}). This database is provided as a monthly grid with a resolution of 1º x 1º. Computed fluxes are based on cloud and aerosol observations from instruments onboard Earth Observing System (EOS) Terra and Aqua satellites and other meteorological assimilation data from the Goddard Earth Observing System (GEOS). Further details about CERES are provided by *Wielicki et al.* [1996]. To compare the monthly anomalies of surface measurements to those computed from 1° by 1° CERES monthly data, the CERES data were interpolated to the locations of the surface measurements using a two-dimensional spatial interpolation from the four closest pixels. A previous comparison [*Kato et al.*, 2013] between CERES and surface-based observations (monthly mean irradiances) from 10 years of data has shown a bias of -1.7 Wm^{-2} and a root mean square error of 13.3 Wm^{-2} in the monthly SSR.

Additional information for this analysis including ozone, water vapor, and surface albedo are obtained using the methodology described by *Mateos et al.* [2013]. Total ozone column and precipitable water column are retrieved from the ERA-Interim reanalysis produced by the European Centre for Medium-Range Weather Forecasts (ECMWF), while monthly land surface albedo is obtained from the MERRA (Modern Era Retrospective-analysis for Research and Applications) reanalysis.

Table 1. Details of the three sites (SSR measurements) used in this study.

Station	Latitude (ºN)	Longitude (ºE)	Altitude (m a.s.l.)	Time period	AERONET Aerosol station
Barcelona	41.39	2.12	125	2004-2012	Barcelona
Valladolid	41.65	-4.77	735	2003-2012	Palencia
Évora	38.57	-7.91	293	2003-2012	Évora

3. Methodology

Radiative flux calculations are required in the evaluation of the radiative effects. Reanalysis information (ozone, water vapor, and surface albedo) and AERONET level 2.0 aerosol data are used as input [see *Valenzuela et al.*, 2012; *Mateos et al.*, 2014; among others] for the libRadtran model [*Mayer and Kylling*, 2005]. The rest of the information required to run the model is the same as explained in detail by *Mateos et al.* [2013]. The simulations are performed each month (with the corresponding monthly means of ozone, aerosols, water vapor, and albedo as input) between 2003 and 2012. Hence, monthly SSR can be estimated under different conditions: $SSR_{cloud\&aer\text{-}free}$ for a cloud- and aerosol-free atmosphere; and $SSR_{cloud\text{-}free}$ for a cloud-free atmosphere (i.e., when aerosol information is used in the model).

With these simulations, the radiative effects of the cloud-aerosol, cloud, and aerosol systems can be derived as [*Ramanathan et al.*, 1989]:

$$CARE = (1 - alb_{sur}) (SSR_{SB} - SSR_{cloud\&aer\text{-}free}) \quad (1)$$

$$CRE = (1 - alb_{sur}) (SSR_{SB} - SSR_{cloud\text{-}free}) \quad (2)$$

$$ARE = (1 - alb_{sur}) (SSR_{cloud\text{-}free} - SSR_{cloud\&aer\text{-}free}) \quad (3)$$

where SSR_{SB} is the surface-based SSR measurement for all-sky conditions.

As can be deduced from the three equations, CARE = CRE + ARE. The separate contribution of clouds and aerosols can be obtained with this method. CRE obtained from this method is also called the surface-based CRE (CRE_{SB}) to distinguish it from CERES data (CRE_{CERES}).

Temporal trends are evaluated following the Sen's slope method and the Mann-Kendall test for significance. In order to remove the seasonal dependence from the results, trends are calculated analyzing the monthly anomalies, which are defined as the difference between the actual value and the corresponding climatic monthly value (i.e., mean of the 10 years analyzed). The trends are obtained in W m^{-2} per year for the analyzed period; however, to simplify the notation of the numbers, the units chosen to show the trends are Wm^{-2} per decade.

4. Results and discussion

4.1. Brightening in the Iberian Peninsula since the 2000s

Satellite derived observations are a useful tool to evaluate global scale SSR trends [e.g., *Pinker et al.*, 2005; *Hatzianastassiou et al.*, 2005; 2012]. In this sense, Figure 1 shows the SSR trends as determined from CERES data on a global basis between 2003 and 2012. Most of the Earth's surface shows small changes of SSR (white areas in Figure 1). However, several parts of the world present large trends, mainly: Brazil, USA, South America, Southern and Eastern Europe, and Oceania. Some regions present SSR changes around +10 W m^{-2} per decade, although extreme values of -20 and over +20 W m^{-2} per decade are also observed. For the latitudinal belt between 60ºS and 60ºN, we obtained an average SSR trend in the period 2003-2012 of +0.4 W m^{-2} per decade using CERES data. At the global scale, a slight BP for SSR is, therefore, observed. The large negative trends shown in Figure 1 in the western Pacific area cannot balance the global SSR increase in this period. *Wild* [2012] reported the average values of SSR trends after 2000 for five different regions by using surface-based observations: USA (+8 Wm^{-2} per decade), Europe (+3 Wm^{-2} per decade), China/Mongolia (-4 Wm^{-2} per decade), Japan (0 Wm^{-2} per decade), and India (-10 Wm^{-2} per decade). Regarding Europe, the value reported by *Wild* [2012] is in line with the majority of the studies reporting SSR trends since the 1980s. In summary, a dimming of SSR is seen in the western Pacific area, while the brightening is observed in the tropical and southeastern Pacific, USA, South America, and Europe. The intensity of the brightening depends on the area and its local conditions. For instance, Table 2 summarizes some of the results of previous studies dealing with the BP in Europe. One of the areas with a notable interest is the Iberian Peninsula (Southwestern Europe) with a recent strong BP that shows higher rates than the surrounding areas.

Table 2. SSR trends for different sites in Europe. More references and regions can be found in the review by Wild (2009).

Reference	SSR trend	Time period	Region
Sanchez-Lorenzo et al. [2013a]	+3.9[a]	1985-2010	Spain
Bilbao et al. [2011]	-15[b]	1991-2000	Central Spain
Bilbao et al. [2011]	+7.5[b]	2001-2010	Central Spain
Wild [2009]	+5[a]	1985-2005	Iberian Peninsula
Wild [2009]	+3.6[a]	1985-2005	France
Ruckstuhl et al. [2008]	+2.6[a]	1981-2005	Switzerland
Ruckstuhl et al. [2008]	+3.3[a]	1981-2005	Northern Germany
Stjern et al. [2009]	+4.4[b]	1983-2003	Northern Europe
Lindfors et al. [2007]	+1.2[b]	1983-2005	Norway
Lindfors et al. [2007]	+4.4[b]	1983-2005	Sweden
Lindfors et al. [2007]	+2.5[b]	1983-2005	Finland
Lindfors et al. [2007]	+3.8[b]	1983-2005	Finland
Sanchez-Lorenzo et al. [2013b]	+4.5[a]	1994-2005	Europe
Chiacchio and Wild [2010]	+0.4[a]	1985-2000	Europe
Hakuba et al. [2013a]	+7.0[a]	2000-2007	Europe
Norris and Wild [2007]	+1.4[a]	1987-2002	Europe

a. W/m2 per decade. b. % per decade

The temporal trends of SSR are established for the period 2003-2012 in the present work for the Iberian Peninsula using data from 15 surface-based stations and are shown in Figure 2a. The spatial interpolation is carried out by an ordinary Kriging method [*Ribeiro et al.*, 2001]. This kind of interpolation is usually carried out with meteorological and atmospheric variables [e.g., *Jolly et al.*, 2005; *Ruiz-Arias et al.*, 2013]. This process is performed with the following characteristics: sill of 10 W^2m^{-4}, range of 3.33º, nugget of 0 W^2m^{-4}, and exponential correlation function. In order to minimize possible uncertainties in the results [e.g., *Yamamoto*, 2000], we decided to limit the discussion of this figure to areas close to each surface-based site. The results are statistically significant (with a level over 90%) for those stations highlighted by a circle. The sites located in the central area of the Iberian Peninsula (Valladolid, Madrid, Logroño, and Albacete) present a strong brightening in SSR with values greater than +10 Wm^{-2} per decade. Large brightening trends are also observed for sites located at the

Mediterranean coast (Málaga and Murcia). The sites at the Atlantic and Cantabric (Northern Iberian Peninsula) coasts exhibit a weaker brightening, although their results are generally not statistically significant. Particularly, only one station, A Coruña (Northwestern coast), shows a negative trend of SSR around -7 W m^{-2} per decade.

In order to corroborate this strong brightening over the Iberian Peninsula, data from CERES over the same period are also analyzed, and the results are presented in Figure 2b. Areas of 1º x 1º showing statistically significant trends are highlighted by circles in Figure 2b. All the central area again presents an enhancement of the SSR over +10 W m^{-2} per decade. We observe good agreement between the surface-based and satellite values. Besides the central area, the trend for the Balearic Islands (Mallorca station) is very similar, and again the trends over the Northern and Western coasts of the peninsula exhibit lower values, in line with the surface-based observations shown in Figure 2a.

Therefore, the intense BP over the Iberian Peninsula between 2003 and 2012 is corroborated by the surface- and satellite- based results in Figure 2 showing trend values greater than +10 W m^{-2} per decade. Table 3 shows the information of the SSR temporal trends over the three sites which are used in the following sections. Considering the other 12 sites shown in Figure 2a, the average rate over the peninsula is +7.0 W m^{-2} per decade (confidence interval of [1.6, 12.9] at the 99% significance level), while the trend for the whole area using CERES data is +6.3 W m^{-2} per decade (confidence interval of [1.6, 11.9] at the 99% significance level). These rates are in line with the values obtained for Barcelona and Évora sites, although smaller than the trend rate for Valladolid. The strong change of SSR levels at Valladolid site was also reported by *Bilbao et al.* [2011] for the decade between 2001 and 2010. Using yearly values of

SSR, they found a trend of 0.75% per year in contrast to the −1.5% per year obtained in the period 1991-2000.

Table 3. Temporal trends for the SSR in three stations of the Iberian Peninsula (units in W m^{-2} per decade); rel.trend is the relative trend with respect to the monthly mean (% per decade), CI is the confidence interval of the trend and SL is the statistical significance level.

Station	SSR trend	rel.trend	CI	SL	Time period
Barcelona	7.6	4.1	[-1.6, 16.7]	88%	2004-2012
Valladolid	12.6	6.7	[4.8, 20.9]	99%	2003-2012
Évora	6.1	3.0	[-4.7,16.6]	70%	2003-2012
Average	7.9	4.1	[0.1,15.3]	96%	2003-2012

4.2. Quantifying the aerosol and cloud effects in the BP

Monthly values of CARE, CRE, and ARE are obtained for the sites Barcelona, Valladolid, and Évora, using the methods described in Section 3. Their temporal evolutions are shown in Figure 3. There are common features for particular periods. For instance, the maximum radiative effects of the clouds-aerosol system (minimum CARE values) obtained in April-2003, May-2008, and April-2012 can be explained by the evolution of clouds since the ARE/CARE ratio is around 0.1, or even less. Hence, clouds explain more than 90% of the CARE values of these peaks (as CARE = CRE + ARE). However, other peaks in May-2004 and April-2007 present a higher contribution of ARE around 20%. The largest ARE values (in absolute term) are obtained in Barcelona, June-2005 and June-2012, with radiative effects around -30 W m^{-2}. For instance, the peak of June-2012 can be explained by the large monthly AOD at 440nm close to 0.4. The CALIMA project (see http://www.calima.ws/) has identified 11 days with Saharan dust intrusions in Northeastern Spain during that month. As a consequence, ARE represents 86% of the CARE value for this month. The stronger aerosol effect in the Barcelona is in line with previous studies which show larger AOD values at this site [e.g., *Mateos et al.*, 2014], and this is expected since Barcelona is a large city. The well known AOD annual cycle with larger values during summer months is translated to an ARE annual cycle. This seasonal pattern is not as evident for CRE values.

Figure 4 presents the histogram of relative frequency of values for the CARE, CRE and ARE for the three stations. Six intervals are selected between -100 and 0 Wm^{-2} at 20 Wm^{-2} steps (e.g., -100 ± 10 Wm^{-2}; -80 ± 10 Wm^{-2};...). As expected from Figure 3, the ARE shows the highest percentage for the smallest (absolute) values (60% of data falling in the interval of 0 ± 10 Wm^{-2}). The maximum contribution of CRE is achieved in the -20 ± 10 Wm^{-2} interval for almost half of the data, although there is also an significant CRE occurrence in the -40 ± 10 Wm^{-2} interval. The maximum occurrence of CARE values (around 40%) is in the interval -40 ±10 Wm^{-2}, but with regard to CARE, the intervals at -60 and -20 Wm^{-2} are also relevant. The magnitude of the values obtained in this study can be compared with the results presented by previous studies (see Table 4). Particularly, ARE values for the three Mediterranean stations (Lampedusa, Valencia, and Granada) are of the same magnitude than the results presented in this study. With respect to CRE, it is very difficult to extract any conclusions since the methodologies to retrieve the cloud radiative effect are very different (using surface-based data, satellite observations, model simulations, or combinations among them); but the values are, in general, similar to what we find here.

Table 4. Range of radiative effects (monthly or annual scale) obtained by previous studies. Units are W m^{-2}.

Reference	Station or Region	ARE values	CRE values	Time period
Chen et al. [2000]	Worldwide	-	(-80, 0)	1989-1993
Gautier and Landsfeld [1997]	Oklahoma (USA)	-	(-90, -22)	1993-1994
Ruckstuhl et al. [2008]	Switzerland	-	(-45, 0)	1981-2005
Dong et al. [2006]	ARM SCF (USA)	-	(-120, -50)	1997–2002
Kim and Ramanathan [2008]	Worldwide	-7	-47	2000-2002
Allan [2011]	Worldwide	-	-52.8	2001-2007
Esteve et al. [2014]	Valencia (Spain)	(-30, 0)	-	2003-2011
Di Biagio et al. [2010]	Lampedusa (Mediterranean)	(-30,0)	-	2004-2007
Valenzuela et al. [2012]	Granada (Spain)	(-35, 0)	-	2005-2011
Pandithurai et al. [2008]	New Delhi	(-100,0)	-	2006
Li et al. [2011]	Worldwide	-	(-400, -50)	2007-2008
García et al. [2014]	Canary Islands	-7	-	2009-2012
Alam et al. [2012]	Pakistan	(-110,-70)	-	2010-2011
Alam et al. [2012]	India	(-80,-50)	-	2010-2011

The temporal evolutions of CARE, CRE, and ARE are analyzed, and the results are summarized in Table 5. On average, the positive trend for CARE is +7.5 W m^{-2} per decade. Note that the average series was built by averaging the monthly anomaly series of each variable (it is not the average of the trends obtained for each series). The average individual trends for CRE and ARE are +5.2 and +1.6 W m^{-2} per decade, respectively. Evaluating the mean contribution of clouds and aerosols to the CARE trend, we can estimate that almost 3/4 of the trend is explained by clouds, while the other 1/4 is due to aerosol changes. The high statistical significance in the three rates for the site Valladolid supports this relevant result. The mean ARE trend of around +2 Wm^{-2} per decade is in line with the cloud-free SSR trends reported in Europe by previous studies [e.g., *Norris and Wild*, 2007; *Ruckstuhl et al.*, 2008]. In particular, *Folini and Wild* [2011] found for the Iberian Peninsula (using the global climate model ECHAM5-HAM) a brightening period between 1989 and 2004 under cloud-free conditions of +1.4 Wm^{-2} per decade, which must be linked to the decrease in the ARE, like in the rest of

Europe. This fact, together with the CRE decrease, has produced the strong increase in SSR since the 2000s in the Iberian Peninsula.

Table 5. Temporal trends of CARE, CRE (both CRE_{SB} and CRE_{CERES}), and ARE. The units for the temporal trends are W m^{-2} per decade, rel.trend is the relative trend with respect to the monthly mean (% per decade), CI is the confidence interval of the trend, SL is the statistical significance level, and C_{CLOUD} and $C_{AEROSOL}$ are the mean contribution of clouds, and aerosols, respectively, to the CARE trend.

		Barcelona	Valladolid	Évora	Average
CARE	trend	7.0	10.2	5.5	7.5
	rel.trend	-15.5	-25.1	-15.4	-18.5
	CI	[-0.8,15.1]	[4.1,16.4]	[-3.0,13.8]	[1.6,13.3]
	SL (%)	91	100	77	99
CRE_{SB}	trend	4.0	7.7	3.3	5.2
	rel.trend	-12.2	-23.9	-11.7	-16.7
	CI	[-4.8,11.8]	[1.6,13.4]	[-5.3,11.1]	[-0.2,11.2]
	SL (%)	58	99	57	94
ARE	trend	2.8	2.0	2.1	1.6
	rel.trend	-22.6	-23.9	-26.7	-17.0
	CI	[1.2,4.3]	[0.4,3.6]	[0.8,3.4]	[0.3,3.0]
	SL (%)	100	95	99	98
C_{CLOUD} (%)		57	75	60	69
$C_{AEROSOL}$ (%)		40	20	38	21
CRE_{CERES}	trend	0.5	2.8	-0.6	-
	rel.trend	-1.3	-7.1	1.9	-
	CI	[-6.6,8.4]	[-2.2,8.0]	[-6.8,5.9]	-
	SL (%)	24	68	19	-

In order to corroborate the decrease in the radiative effects of clouds and aerosols over the Iberian Peninsula in the last decade, the temporal trends of cloud observations, aerosol optical depth at 440 nm (AOD_{440nm}), and particulate matter under 10 µm (PM_{10}) are also analyzed. The AEMET database also contains visual observations of total cloud cover (TCC) three times per day (6, 12, and 18h GMT) [*Mateos et al.*, 2010; *Sanchez-Lorenzo et al.*, 2012]. With the three observations in oktas, the daily averages are evaluated as percentage of sky covered by clouds (1 okta = 12.5%). Then, monthly values are used to identify the trends in three sites close to the stations analyzed in this study: Valladolid airport (Valladolid), Barcelona airport (Barcelona), and Badajoz (Évora). Aerosol AERONET stations are the same as mentioned in Section 2. It is worth mentioning here that in a previous paper, *Mateos et al.* [2014] observed a decreasing trend in yearly AOD values over the whole Iberian Peninsula around -0.04 AOD_{500nm}-unit per decade. In the same study, the site Barcelona exhibited a statistically significant trend of -0.09 AOD_{440nm}-unit per decade (2004-2012 period). This rate is stronger than the average decrease in AOD of around -0.04 AOD_{440nm}-unit per decade reported over the Euro-Mediterranean region from 1979 and 2009 using satellite and model data [*Nabat et al.*, 2013]. In two sites of the western Mediterranean, Avignon (France) and Ispra (Italy), the AOD trends are insignificant or decreasing in the early 2000s [*Yoon et al.*, 2012]. In the present study, the monthly database described above is used for this purpose. The results are similar to those obtained by *Mateos et al.* [2014], although the use of a monthly scale adds more significance level to the results. To reinforce the aerosol trends, the more stable database of particulate matter given by PM_{10} is used. PM data are recorded under all-sky conditions, in contrast to AOD observations which are obtained under cloud-free conditions. In a recent paper focusing on the Palencia-AERONET site, *Bennouna et al.* [2014] have shown the influence of sampling on the PM-AOD relationship and trends, corroborating AOD trends based on the more stable PM series. The PM_{10} sites used in this study are: the European Monitoring and Evaluation Programme (EMEP) database [*Aas et al.*, 2013] for Valladolid (Peñausende site) and Évora (Barcarrota site); and for the Barcelona station the site of Castellbisball (managed by Generalitat de Catalunya) is selected to present the evolution of PM_{10} over that area. This choice is justified because this site can be considered as background for the urban conditions in the Barcelona area. The temporal trends for all these variables and stations are computed following the same methodology that was explained in Section 3. The results are summarized in Table 6.

In the Valladolid region, a strong decrease in the cloud cover (-24% per decade) is observed during the analyzed period, which is in line with the large positive CRE trend shown in Table 5. This fact has produced, together with a reduction of the aerosol load (-18% per decade), one of the largest recent BP over the Iberian Peninsula. The reduction in the atmospheric aerosols in this period is corroborated by the negative trends observed in PM_{10} and AOD_{440nm}. Barcelona station presents the largest negative trend for AOD_{440nm} (-0.06 AOD-unit per decade), which is in line with the slightly more positive trend observed in Table 5 for ARE (+2.8 Wm^{-2} per decade). The difference between Barcelona and the other two sites for the PM_{10} results is based on the suburban characteristics of Castellbisball site. The other two sites considered (Peñausende and Barcarrota) are rural, and therefore, represent background aerosols. Local regulations to reduce air pollution in urban environments and the impact of the current economic crisis have produced this large decline of the particulate matter [e.g., *Cusack et al.*, 2012; *Querol et al.*, 2014]. Furthermore, natural aerosols such as intense desert dust events (AOD at 550nm over 0.4) are found to decrease in the western Mediterranean Basin between 2000 and 2007 [*Gkikas et al.*, 2013]. The decreases of cloud cover are slightly smaller for Évora and notably lower for Barcelona, but the low statistical significance of these results for CRE make it difficult to draw firm conclusions for these sites. ARE trends are similar for the three stations (between -0.06 and -0.03 AOD-unit per decade), hence the differences in the SSR trends can be understood as differences in the temporal evolution of the local cloud cover (between -9.4 and -3.2 % per decade). Overall, the decreases of total cloud cover and aerosol load over the Iberian Peninsula seem to corroborate the strong BP during the last decade.

Table 6. Temporal trends of several variables between 2003 and 2012; rel.trend is the relative trend with respect to the mean monthly value, CI is the confidence interval of the trend, SL is the statistical significance level.

		Barcelona	Valladolid	Évora
TCC	trend[a]	-3.2	-9.4	-6.6
	rel.trend[a]	-8.5	-23.8	-20.0
	CI[a]	[-6.9,0.8]	[-13.3,-5.3]	[-11.9,-1.5]
	SL (%)	85	100	94
PM_{10}	trend[b]	-18.4	-4.7	-3.3
	rel.trend[a]	-54.2	-43.9	-21.0
	CI[b]	[-23.7,-13.6]	[-6.4,-3.0]	[-6.0,-0.1]
	SL (%)	100	100	99
AOD_{440nm}	trend[c]	-0.06	-0.03	-0.04
	rel.trend[a]	-27.8	-18.4	-29.3
	CI[c]	[-0.08, -0.03]	[-0.05,-0.01]	[-0.06,-0.02]
	SL (%)	100	97	100

a) units in % per decade. b) units in µg/m3 per decade. c) units in AOD-unit per decade

4.3. CRE comparison between CERES and surface-based data

The estimations of CRE performed by CERES instrument (CRE_{CERES}) can help to assess the robustness of the proposed method (CRE_{SB}). Figure 5 shows the monthly evolution of both CRE series. A good agreement can be observed between them because the two series follow the same pattern and reproduce the same peaks with a similar magnitude. To minimize the impact of the seasonal dependence on this comparison, the monthly CRE anomalies are used to establish a linear relationship (see Figure 6) between both methods. The results show a good agreement between CRE from CERES EBAF-Surface and from the method presented in this study.

Nevertheless, the trends calculated from CERES EBAF-Surface are notably smaller than those presented for CRE_{SB} (see Table 5). Actually, CRE_{CERES} trends indicate no change and slight decrease for the cloud radiative effects in Barcelona and Évora, respectively, although with very low statistical significance. The results for Valladolid site exhibit the highest reduction of cloud effects, which is again linked to the strong BP observed over this station. The differences in the temporal trends can be understood due to two possible reasons: a) the spatial representativeness of 1º x 1º grid as compared to local data [e.g., *Hakuba et al.*, 2013b], which can produce several uncertainties because it is possible that non-homogeneous clouds (non-spatially continuous or different types/levels) can exist in that area; and b) artificial trends in the evaluation of surface clear-sky SSR flux caused by the two versions of satellite aerosol products used in the CERES_EBAF-Surface_Ed2.7 dataset (see the Data Quality Summary, June 7 2013, https://eosweb.larc.nasa.gov/). Looking again at Table 6, the observed trends for TCC over the three stations are in line with those trends obtained for CRE_{SB}. Therefore, CRE_{CERES} and CRE_{SB} are in agreement, but some kind of uncertainty is observed regarding temporal trends.

5. Conclusions

Monthly surface shortwave radiation (SSR) data from three surface-based sites (Barcelona, Valladolid, and Évora) of the Iberian Peninsula between 2003 and 2012, and simulations under cloud-free and cloud- and aerosol-free conditions by the libRadtran model are used to obtain the cloud-aerosol (CARE), cloud (CRE), and aerosol (ARE) radiative effects separately. The simulations are performed considering, among other data, aerosol information from AERONET stations. CERES data are used to corroborate the surface-based findings. The main conclusions obtained in this study are summarized next:

1) A strong brightening phenomenon is observed in the Iberian Peninsula in the early 2000s, around +7 Wm^{-2} between 2003 and 2012 corroborated by surface-based and satellite data. The central area presents an SSR trend (significance level >90%) greater than 10 Wm^{-2} per decade. Large trends are also observed in the eastern area. However, the west and northwest areas show weaker trends with values near zero and even negative.

2) More than 95% of the CARE values in these stations and time period range between -90 and -10 Wm^{-2}. A similar amount of CRE data is between -70 and 0 Wm^{-2}, and between -30 and 0 Wm^{-2} for ARE.

3) On average, CARE, CRE, and ARE trends exhibit rates of +7, +5, and +2 Wm^{-2} over the 2003-2012 period, respectively. Therefore, three-fourths of the SSR trend is explained by clouds, while the other one-fourth is due to aerosol changes in this period.

4) The increase of the SSR radiation levels is consistent with the reductions in total cloud cover, PM_{10}, and columnar aerosol load in the three sites of study.

5) CERES CRE estimations show good agreement with the surface-based data, although some discrepancies are observed in the evaluation of temporal trends.

The method proposed in this study can be applied to solar radiation databases (such as Global Energy Balance Archive, GEBA) which present both large spatial and long temporal coverage to obtain the separate contribution of clouds and aerosols in other worldwide regions during the last decades.

Acknowledgments

We thank the Spanish Meteorological Agency (AEMET) for providing the surface solar radiation and cloud cover data. We thank the PI investigators and their staff for establishing and maintaining the RIMA/PHOTONS sites of Palencia, Barcelona, and Évora, belonging to AERONET-EUROPE network. The authors also acknowledge the project and support of the European Community - Research Infrastructure Action under the FP7 "Capacities" specific program for Integrating Activities, ACTRIS Grant Agreement no. 262254. CERES data were obtained from the NASA Langley Research Center Atmospheric Science Data Center. We would like to acknowledge EMEP for allowing free access to ambient PM levels recorded at a large number of sites in the Iberian Peninsula. PM10 levels for stations around Barcelona were kindly provided by David Pagès from the Xarxa de Vigilància i Previsió de la Contaminació Atmosfèrica (XVPCA) from the Generalitat de Catalunya. ECMWF ERA-Interim data used in this study have been obtained from the ECMWF data server: http://data.ecmwf.int/data. Analyses and visualizations of MERRA data used in this paper were produced with the Giovanni online data system, developed and maintained by the NASA GES DISC. Manuel Antón thanks Ministerio de Ciencia e Innovación and Fondo Social Europeo for the award of a postdoctoral grant (Ramón y Cajal). Arturo Sanchez-Lorenzo thanks the “Secretaria per a Universitats i Recerca del Departament d'Economia i Coneixement, de la Generalitat de Catalunya i del programa Cofund de les Accions Marie Curie del 7è Programa marc d'R+D de la Unió Europea” (2011BP-B00078) and the postdoctoral fellowship #JCI-2012-12508. Financial support to the University of Valladolid was provided by the Spanish MINECO (Ref. Projects CGL2011-23413 and CGL2012-33576). Josep Calbó is supported by the Spanish Ministry of Science and Innovation project NUCLIERSOL (CGL2010-18546). University of Extremadura thanks the supported by MINECO (ref. CGL2011-29921-C02-01). M. J. Costa thanks the funding provided by the Évora Geophysics Centre, Portugal, under the contract with FCT (the Portuguese Science and Technology Foundation), PEst-OE/CTE/UI0078/2014.

References

Aas, W., et al. (2013), Transboundary particulate matter in Europe Status report 2013, *EMEP Report*, *4/2013* (Ref. O-7726), ISSN: 1504-6109 (print), 1504-6192 (online).

Alam, K., T. Trautmann, T. Blaschke, and H. Majid (2012), Aerosol optical and radiative properties during summer and winter seasons over Lahore and Karachi, *Atmos. Environ., 50*, 234–245.

Allan, R.P. (2011), Combining satellite data and models to estimate cloud radiative effect at the surface and in the atmosphere, *Meteorol. Appl., 18*, 324-333. doi: 10.1002/met.285.

Antón, M., and D. Mateos (2013), Shortwave radiative forcing due to long-term changes of total ozone column over the Iberian Peninsula, *Atmos. Environ., 81*, 532-537, doi: 10.1016/j.atmosenv.2013.09.047.

Augustine, J. A., and E. G. Dutton (2013), Variability of the surface radiation budget over the United States from 1996 through 2011 from high-quality measurements, J. Geophys. Res. Atmos., 118, 43–53, doi:10.1029/2012JD018551.

Bennouna, Y.S., V. Cachorro, M.A. Burgos, C. Toledano, B. Torres, and A. de Frutos (2014), Relationships between columnar aerosol optical properties and surface Particulate Matter observations in north-central Spain from long-term records (2003-2011), *Atmos. Meas. Tech. Discuss., 7,* 5829–5882, doi:10.5194/amtd-7-5829-2014.

Bilbao, J., R. Roman, A. de Miguel, and D. Mateos (2011), Long-term solar erythemal UV irradiance data reconstruction in Spain using a semiempirical method, *J. Geophys. Res.*, *116*, D22211, doi:10.1029/2011JD015836.

Chen, T., W.B. Rossow, and Y. Zhang (2000), Radiative Effects of Cloud-Type Variations, *J. Climate*, *13*, 264-286.

Chiacchio, M., and M. Wild (2010), Influence of NAO and clouds on long-term seasonal variations of surface solar radiation in Europe, *J. Geophys. Res.*, *115*, D00D22, doi:10.1029/2009JD012182.

Chiacchio, M., and R. Vitolo (2012), Effect of cloud cover and atmospheric circulation patterns on the observed surface solar radiation in Europe, J. Geophys. Res., 117, D18207, doi:10.1029/2012JD017620.

Cusack, M., A. Alastuey, N. Pérez, J. Pey, and X. Querol (2012), Trends of particulate matter ($PM_{2.5}$) and chemical composition at a regional background site in the Western Mediterranean over the last nine years (2002–2010), *Atmos. Chem. Phys.*, *12*, 8341-8357, doi:10.5194/acp-12-8341-2012.

Di Biagio, C., A. di Sarra, and D. Meloni (2010), Large atmospheric shortwave radiative forcing by Mediterranean aerosols derived from simultaneous ground-based and spaceborne observations and dependence on the aerosol type and single scattering albedo, *J. Geophys. Res.*, *115,* D10209, doi:10.1029/2009JD012697, 2010.

Dong, X., B. Xi, and P. Minnis (2006), A Climatology of Midlatitude Continental Clouds from the ARM SGP Central Facility. Part II: cloud fraction and surface radiative forcing, *J. Climate*, *19*, 1765-1782.

Esteve, A.R., V. Estellés, M.P. Utrillas, and J.A. Martínez-Lozano (2014), Analysis of the aerosol radiative forcing over a Mediterranean urban coastal site, *Atmos. Res.*, *137,* 194-204, http://dx.doi.org/10.1016/j.atmosres.2013.10.009.

Folini, D., and M. Wild (2011), Aerosol emissions and dimming/brightening in Europe: Sensitivity studies with ECHAM5‐HAM, *J. Geophys. Res., 116*, D21104, doi:10.1029/2011JD016227.

Gautier, C. and M. Landsfeld (1997), Surface solar radiation flux and cloud radiative forcing for the Atmospheric Radiation Measurement (ARM) Southern Great Plains (SGP): a satellite, surface observations, and radiative transfer model study, *J. Atmos. Sci.*, 54(10), 1289-1307.

Garcia, R.D., O.E. Garcia, E. Cuevas, V.E. Cachorro, P.M. Romero-Campos, R. Ramos, and A.M. de Frutos (2014), Solar radiation measurements compared to simulations at the BSRN Izana station: Mineral dust radiative forcing and efficiency study, *J. Geophys. Res. Atmos.*, *119*, doi:10.1002/2013JD020301.

Gkikas, A., N. Hatzianastassiou, M. Mihalopoulos, V. Katsoulis, S. Kazadzis, J. Pey, X. Querol, and O. Torres (2013). The regime of intense desert dust episodes in the Mediterranean based on contemporary satellite observations and ground measurements, *Atmos. Chem. Phys., 13,* 12135-12154, doi:10.5194/acp-13-12135-2013.

Hakuba, A., A. Sanchez-Lorenzo, D. Folini, and M. Wild (2013a), Testing the Homogeneity of Short-Term Surface Solar Radiation Series in Europe, *AIP Conference Proceedings, 1531*, 700, doi: 10.1063/1.4804866.

Hakuba, M.Z., D. Folini, A. Sanchez-Lorenzo, and M. Wild (2013b), Spatial representativeness of ground-based solar radiation measurements, J. Geophys. Res. Atmos.,118, 8585–8597, doi:10.1002/jgrd.50673.

Hatzianastassiou, N., C. Matsoukas, A. Fotiadi, K.G. Pavlakis, E. Drakakis, D. Hatzidimitriou, and I. Vardavas (2005), Global distribution of Earth's surface shortwave radiation budget, *Atmos. Chem. Phys., 5*, 2847-2867, doi:10.5194/acp-5-2847-2005.

Hatzianastassiou, N., C.D. Papadimas, C. Matsoukas, K. Pavlakis, A. Fotiadi, M. Wild, and I. Vardavas (2012), Recent regional surface solar radiation dimming and brightening patterns: inter-hemispherical asymmetry and a dimming in the Southern Hemisphere. *Atmosph. Sci. Lett., 13*, 43–48. doi: 10.1002/asl.361.

Holben, B.N., et al. (1998), AERONET – A federated instrument network and data archive for aerosol characterization, *Rem. Sen. Environ., 66*, 1–16.

Jolly, W.M., J.M. Graham, A. Michaelis, R. Nemani, and S.W. Running (2005), A flexible, integrated system for generating meteorological surfaces derived from point sources across multiple geographic scales, *Environ. Modell. Softw., 20*, 873-882, doi:10.1016/j.envsoft.2004.05.003.

Kato, S., N.G. Loeb, F.G. Rose, D.R. Doelling, D.A. Rutan, T.E. Caldwell, L.S. Yu, R.A. Weller (2013), Surface irradiances consistent with ceres-derived top-of-atmosphere shortwave and longwave irradiances. *J. Clim.*, 26(9), 2719-2740. doi: 10.1175/Jcli-D-12-00436.

Kawamoto, K., and T. Hayasaka (2012), Cloud and aerosol contributions to variation in shortwave surface irradiance over East Asia in July during 2001 and 2007, *J. Quant. Spectrosc. Ra., 112,* 329–337, doi:10.1016/j.jqsrt.2010.08.002.

Kim, D., and V. Ramanathan (2008), Solar radiation budget and radiative forcing due to aerosols and clouds, *J. Geophys. Res., 113*, D02203, doi:10.1029/2007JD008434.

Kudo, R., A. Uchiyama, O. Ijima, N. Ohkawara, and S. Ohta (2012), Aerosol impact on the brightening in Japan, *J. Geophys. Res., 117*, D07208, doi:10.1029/2011JD017158.

Kvalevag, M. M., and G. Myhre (2007), Human impact on direct and diffuse solar radiation during the industrial era, *J. Climate.*, 20, 4874– 4883, doi:10.1175/JCLI4277.1.

Li, J., Y. Yi, P. Minnis, J. Huang, H. Yan, Y. Ma, W. Wang, and J.K. Ayers (2011), Radiative effect differences between multi-layered and single-layer clouds derived from CERES, CALIPSO, and CloudSat data, *J. Quant. Spectrosc. Ra., 112*, 361-375, doi:10.1016/j.jqsrt.2010.10.006.

Liley, J. B. (2009), New Zealand dimming and brightening, J. Geophys. Res., 114, D00D10, doi:10.1029/2008JD011401.

Lindfors, A., J. Kaurola, A. Arola, T. Koskela, K. Lakkala, W. Josefsson, J. A. Olseth, and B. Johnsen (2007), A method for reconstruction of past UV radiation based on radiative transfer modeling: Applied to four stations in northern Europe, *J. Geophys. Res., 112,* D23201, doi:10.1029/2007JD008454.

Long, C. N., E. G. Dutton, J. A. Augustine, W. Wiscombe, M. Wild, S. A. McFarlane, and C. J. Flynn (2009), Significant decadal brightening of downwelling shortwave in the continental United States, *J. Geophys. Res., 114*, D00D06, doi:10.1029/2008JD011263

Mateos, D., J. Bilbao, A. de Miguel, and A. Perez-Burgos (2010), Dependence of ultraviolet (erythemal and total) radiation and CMF values on total and low cloud covers in Central Spain, *Atmos. Res., 98,* 21‑27, doi:10.1016/j.atmosres.2010.05.002.

Mateos, D., M. Antón, A. Sanchez-Lorenzo, J. Calbó, and M. Wild (2013), Long-term changes in the radiative effects of aerosols and clouds in a mid-latitude region (1985–2010), *Global Planet. Change, 111*, 288-295, http://dx.doi.org/10.1016/j.gloplacha.2013.10.004.

Mateos, D., M. Antón, C. Toledano, V.E. Cachorro, L. Alados-Arboledas, M. Sorribas, M.J. Costa, and J.M. Baldasano (2014), Aerosol radiative effects in the ultraviolet, visible, and near-infrared spectral ranges using long-term aerosol data series over the Iberian Peninsula, *Atmos. Chem. Phys. Discuss.*, *14*, 1–39, doi:10.5194/acpd-14-1-2014.

Mayer, B., and A. Kylling (2005), Technical note: The libRadtran software package for radiative transfer calculations - description and examples of use, *Atmos. Chem. Phys.*, *5*, 1855-1877, doi:10.5194/acp-5-1855-2005.

Nabat, P. et al. (2013), A 4-D climatology (1979–2009) of the monthly tropospheric aerosol optical depth distribution over the Mediterranean region from a comparative evaluation and blending of remote sensing and model products, *Atmos. Meas. Tech.*, *6*, 1287-1314.

Niemeier, U., H. Schmidt, K. Alterskjær, and J. E. Kristjánsson (2013), Solar irradiance reduction via climate engineering: Impact of different techniques on the energy balance and the hydrological cycle, *J. Geophys. Res. Atmos.*, *118*, 11,905–11,917, doi:10.1002/2013JD020445.

Norris, J. R., and M. Wild (2007), Trends in aerosol radiative effects over Europe inferred from observed cloud cover, solar ‘‘dimming,’’ and solar ‘‘brightening,’’ *J. Geophys. Res.*, *112*, D08214, doi:10.1029/2006JD007794.

Norris, J. R., and M. Wild (2009), Trends in aerosol radiative effects over China and Japan inferred from observed cloud cover, solar ‘dimming’ and solar ‘brightening’, *J. Geophys. Res.*, *114*, D00D15, doi:10.1029/2008JD011378.

Pandithurai, G., S. Dipu, K. K. Dani, S. Tiwari, D. S. Bisht, P. C. S. Devara, and R. T. Pinker (2008), Aerosol radiative forcing during dust events over New Delhi, India, *J. Geophys. Res.*, *113*, D13209, doi:10.1029/2008JD009804.

Pinker, R. T., B. Zhang, and E. G. Dutton (2005), Do satellites detect trends in surface solar radiation? *Science, 308*, 850– 854.

Philipona, R., K. Behrens, and C. Ruckstuhl (2009), How declining aerosols and rising greenhouse gases forced rapid warming in Europe since the 1980s, *Geophys. Res. Lett.*, *36*, L02806, doi:10.1029/2008GL036350.

Querol, X., et al. (2014), 2001-2012 trends on air quality in Spain, *Sci. Total Environ.*, *490*, 957-969.

Ramanathan, V., and G. Carmichael (2008), Global and regional climate changes due to black carbon. *Nat. Geosci., 1,* 221–227.

Ramanathan, V., R.D. Cess, E.F. Harrison, P. Minnis, B.R. Barkstrom, E. Ahmad, and D. Hartmann (1989), Cloud-Radiative Forcing and Climate: Results from the Earth Radiation Budget Experiment, *Science, 243(4887)*, 57–63.

Ribeiro Jr., P.J., and P.J. Diggle (2001), geoR: A package for geostatistical analysis. *R-News* 1(2), 15-18, ISSN 1609-3631.

Ruckstuhl, C., et al. (2008), Aerosol and cloud effects on solar brightening and the recent rapid warming, *Geophys. Res. Lett.*, *35*, L12708, doi:10.1029/2008GL034228.

Ruckstuhl, C., and J. R. Norris (2009), How do aerosol histories affect solar 'dimming' and 'brightening' over Europe?: IPCC-AR4 models versus observations, *J. Geophys. Res., 114,* D00D04, doi:10.1029/2008JD011066

Ruckstuhl, C., J. R. Norris, and R. Philipona (2010), Is there evidence for an aerosol indirect effect during the recent aerosol optical depth decline in Europe?, *J. Geophys. Res., 115,* D04204, doi:10.1029/2009JD012867.

Ruiz-Arias, J.A., J. Dudhia, V. Lara-Fanego, and D. Pozo-Vázquez (2013), A geostatistical approach for producing daily Level-3 MODIS aerosol optical depth analyses, Atmos. Env., 79, 395-405.

Sanchez-Lorenzo, A., J. Calbo, and M. Wild (2012), Increasing cloud cover in the 20th century: review and new findings in Spain, *Clim. Past, 8,* 1199-1212.

Sanchez-Lorenzo, A., J. Calbó, and M. Wild (2013a), Global and diffuse solar radiation in Spain: Building a homogeneous dataset and assessing trends, *Global Planet. Change, 100,* 343-352, http://dx.doi.org/10.1016/j.gloplacha.2012.11.010.

Sanchez-Lorenzo, A., M. Wild, and J. Trentmann (2013b), Validation and stability assessment of the monthly mean CM SAF surface solar radiation dataset over Europe against a homogenized surface dataset (1983–2005), *Remote. Sens. Environ., 134,* 355–366.

Stanhill, G. and S. Cohen (2001), Global dimming: a review of the evidence for a widespread and significant reduction in global radiation with discussion of its probable causes and possible agricultural consequences, *Agr. Forest Meteorol., 107,* 255-278.

Stephens, G.L., J. Li, M. Wild, C.A. Clayson, N. Loeb, S. Kato, T. L'Ecuyer, P.W. Stackhouse Jr., M. Lebsock, and T. Andrews (2012), An update on Earth's energy balance in light of the latest global observations, *Nature Geosci., 5,* 691–696.

Stjern, C.W., J.E. Kristjansson, and A.W. Hansen (2009), Global dimming and global brightening: an analysis of surface radiation and cloud cover data in northern Europe, *Int. J. Climatol., 29,* 643–653.

Toledano, C., V.E. Cachorro, A. Berjon, A.M. de Frutos, M. Sorribas, B. de la Morena, and P. Goloub (2007), Aerosol optical depth and Ångström exponent climatology at El Arenosillo AERONET site (Huelva, Spain), *Q. J. R. Meterol. Soc., 133,* 795-807.

Trenberth, K.E., J.T. Fasullo, J. Kiehl (2009), Earth's global energy budget, *B. Am. Meteorol. Soc., 90(3),* 311–323.

Valenzuela, A., F.J. Olmo, H. Lyamani, M. Antón, A. Quirantes, L. and Alados-Arboledas (2012), Aerosol radiative forcing during African desert dust events (2005-2010) over Southeastern Spain, *Atmos. Chem. Phys.*, *12*, 10331–10351, doi:10.5194/acp-12-10331-2012.

Wang, Y.W. and Y.H. Yang (2014), China's dimming and brightening: evidence, causes and hydrological implications, *Ann. Geophys.*, *32*, 41-55, doi:10.5194/angeo-32-41-2014, 2014.

Wielicki, B.A., B.R. Barkstrom, E.F. Harrison, R.B. Lee III, G.L. Smith, and J.E. Cooper (1996), Clouds and the Earth's Radiant Energy System (CERES): An Earth Observing System Experiment, *B. Am. Meteorol. Soc.*, *77*, 853-868.

Wild, M., H. Gilgen, A. Roesch, A. Ohmura, C.N. Long, E.G. Dutton, B. Forgan, A. Kallis, V. Russak, A. Tsvetkov (2005), From dimming to brightening: decadal changes in surface solar radiation, *Science*, *308*, 847–850.

Wild, M. (2009), Global dimming and brightening: a review, *J. Geophys. Res. 114*, D00D16. http://dx.doi.org/10.1029/2008JD011470.

Wild, M. (2012), Enlightening global dimming and brightening. *Bull. Am. Meteorol. Soc.*, *93*, 27–37, doi:10.1175/BAMS-D-11-00074.1.

Wild, M., D. Folini, C. Schaer, N. Loeb, E.G. Dutton, G. Koning-Langlo (2013), The global energy balance from a surface perspective. *Clim. Dynam.*, *40,* 3107-3134 , http://dx.doi.org/10.1007/s00382-012-1569-8.

Willmott, C. J. (1982), Some Comments on the Evaluation of Model Performance, *Bull. Am. Meteorol. Soc.*, *63*, 1309–1313.

Yamamoto, J.H. (2000), An alternative measure of the reliability of ordinary Kriging estimates, Math. Geol., 32, 489-509.

Yang, W.J., K. Yang, J. Qin, C.C.K. Cheng, and J. He (2011), Solar radiation trend across China in recent decades: a revisit with quality-controlled data, *Atmos. Chem. Phys., 11*, 393-406, doi:10.5194/acp-11-393-2011.

Yoon, J., W. von Hoyningen-Huene, A.A. Kokhanovsky, M. Vountas, and J. Burrows (2012), Trend analysis of aerosol optical thickness and Ångström exponent derived from the global AERONET spectral observations, *Atmos. Meas. Tech., 5*, 1271-1299, doi:10.5194/amt-5-1271-2012.

Figure Captions

Figure 1. Surface shortwave radiation trends between 2003 and 2012 (in W m^{-2} per decade) using CERES (Clouds and the Earth's Radiant Energy System)-EBAF (Energy Balanced And Filled)-Surface data (Kato et al., 2013).

Figure 2. Surface shortwave radiation trends (in W m^{-2} per decade) between 2003 and 2012 over the Iberian Peninsula using surface -based (a) and CERES (Clouds and the Earth's Radiant Energy System)-EBAF (Energy Balanced And Filled)-Surface (b) data. Circles highlight the areas with a statistically significance level over 90% and symbols point out the sites where the trends were calculated (squares are Barcelona, Valladolid, and Évora sites, while triangles are the rest of the stations).

Figure 3. Monthly evolution of radiative effects of aerosols, ARE (a), clouds, CRE (b), and clouds and aerosols, CARE (c), at the sites Barcelona (blue diamonds), Valladolid (black triangles), and Évora (red circles).

Figure 4. Relative frequency of aerosol (ARE), cloud (CRE), and cloud and aerosol (CARE) radiative effects occurrence for the three sites analyzed in this study.

Figure 5. Monthly evolution of cloud radiative effect (CRE) using the method presented in this article (CRE_{SB}, solid symbols) and the estimations given by CERES (Clouds and the Earth's Radiant Energy System)-EBAF (Energy Balanced And Filled)-Surface (CRE_{CERES}, open squares).

Figure 6. Scatter plot of cloud radiative effect monthly anomalies by the estimations given by CERES (Clouds and the Earth's Radiant Energy System)-EBAF (Energy Balanced And Filled)-Surface (CRE_{CERES}) and by the method presented in this article (CRE_{SB}). The solid line points out the linear fit, and the dashed line is the 1:1 line. Legend: n (number of data), mbe (mean bias error), mabe (mean

absolute bias error), rmse (root mean square error), i_{agree} (index of agreement) [*Willmott*, 1982], and R (correlation coefficient).

Figures + Figure Captions

Figure 1

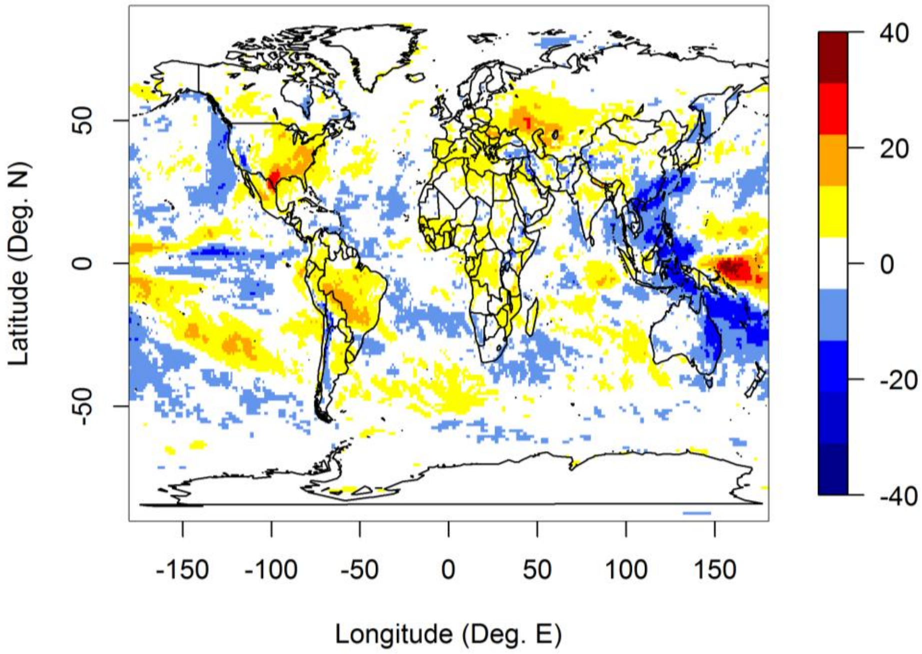

Figure 1. Surface shortwave radiation trends between 2003 and 2012 (in W m^{-2} per decade) using CERES (Clouds and the Earth's Radiant Energy System)-EBAF (Energy Balanced And Filled)-Surface data (Kato et al., 2013).

Figure 2

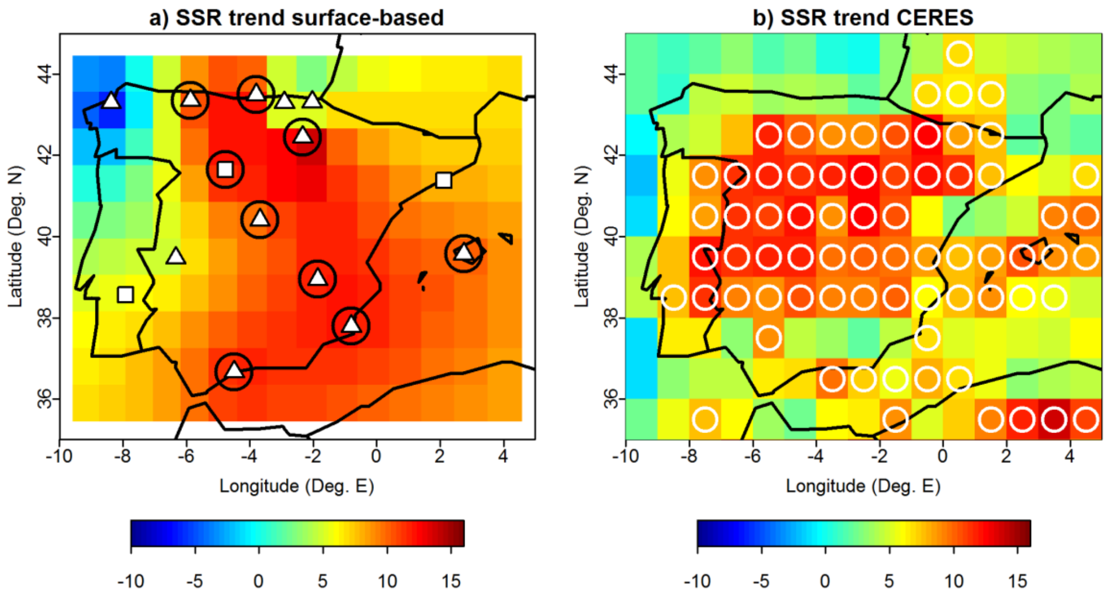

Figure 2. Surface shortwave radiation trends (in W m^{-2} per decade) between 2003 and 2012 over the Iberian Peninsula using surface-based (a) and CERES (Clouds and the Earth's Radiant Energy System)-EBAF (Energy Balanced And Filled)-Surface (b) data. Circles highlight the areas with a statistically significance level over 90% and symbols point out the sites where the trends were calculated (squares are Barcelona, Valladolid, and Évora sites, while triangles are the rest of the stations).

Figure 3

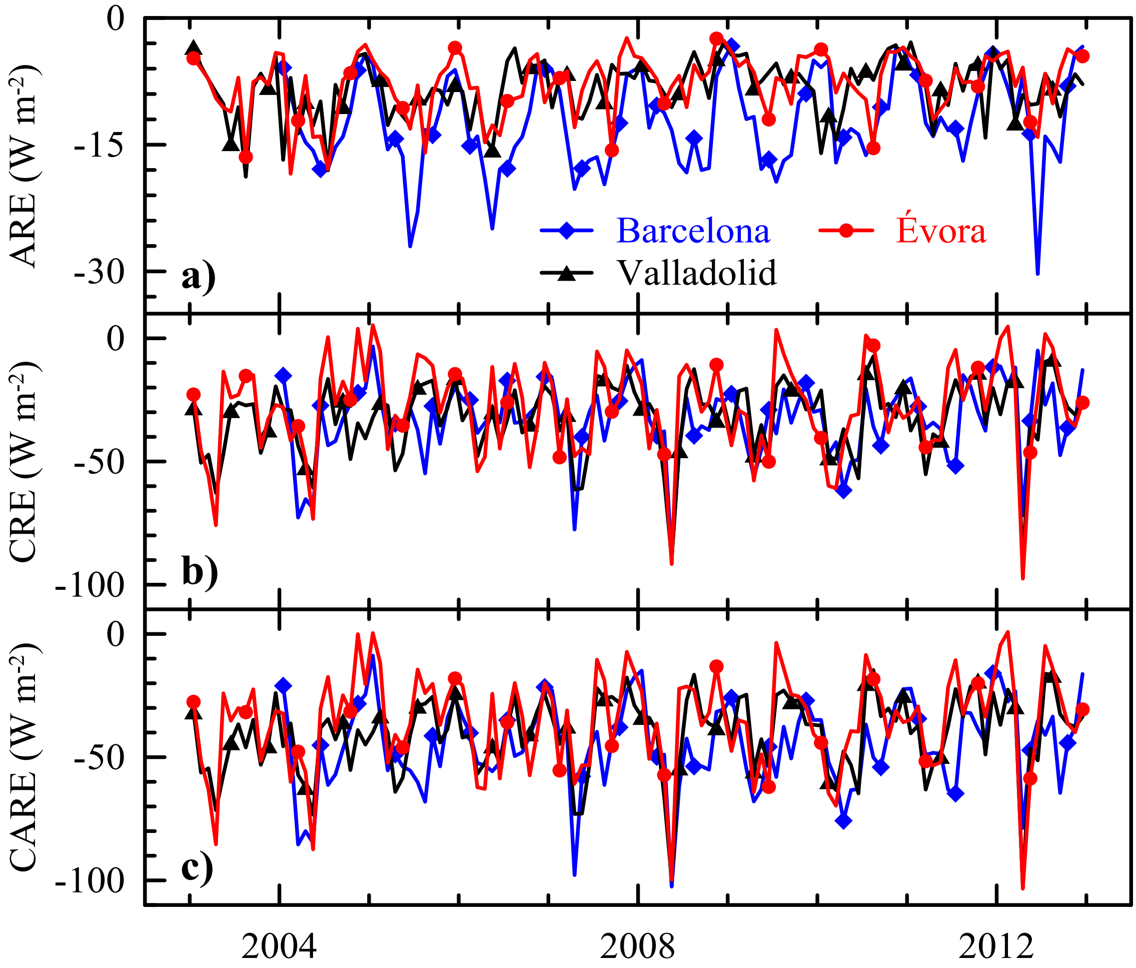

Figure 3. Monthly evolution of radiative effects of aerosols, ARE (a), clouds, CRE (b), and clouds and aerosols, CARE (c), at the sites Barcelona (blue diamonds), Valladolid (black triangles), and Évora (red circles).

Figure 4

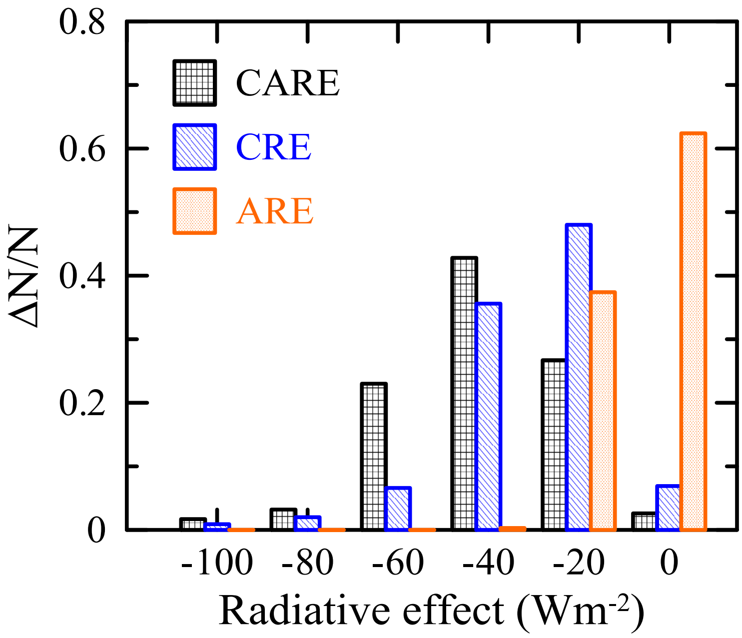

Figure 4. Relative frequency of aerosol (ARE), cloud (CRE), and cloud and aerosol (CARE) radiative effects occurrence for the three sites analyzed in this study.

Figure 5

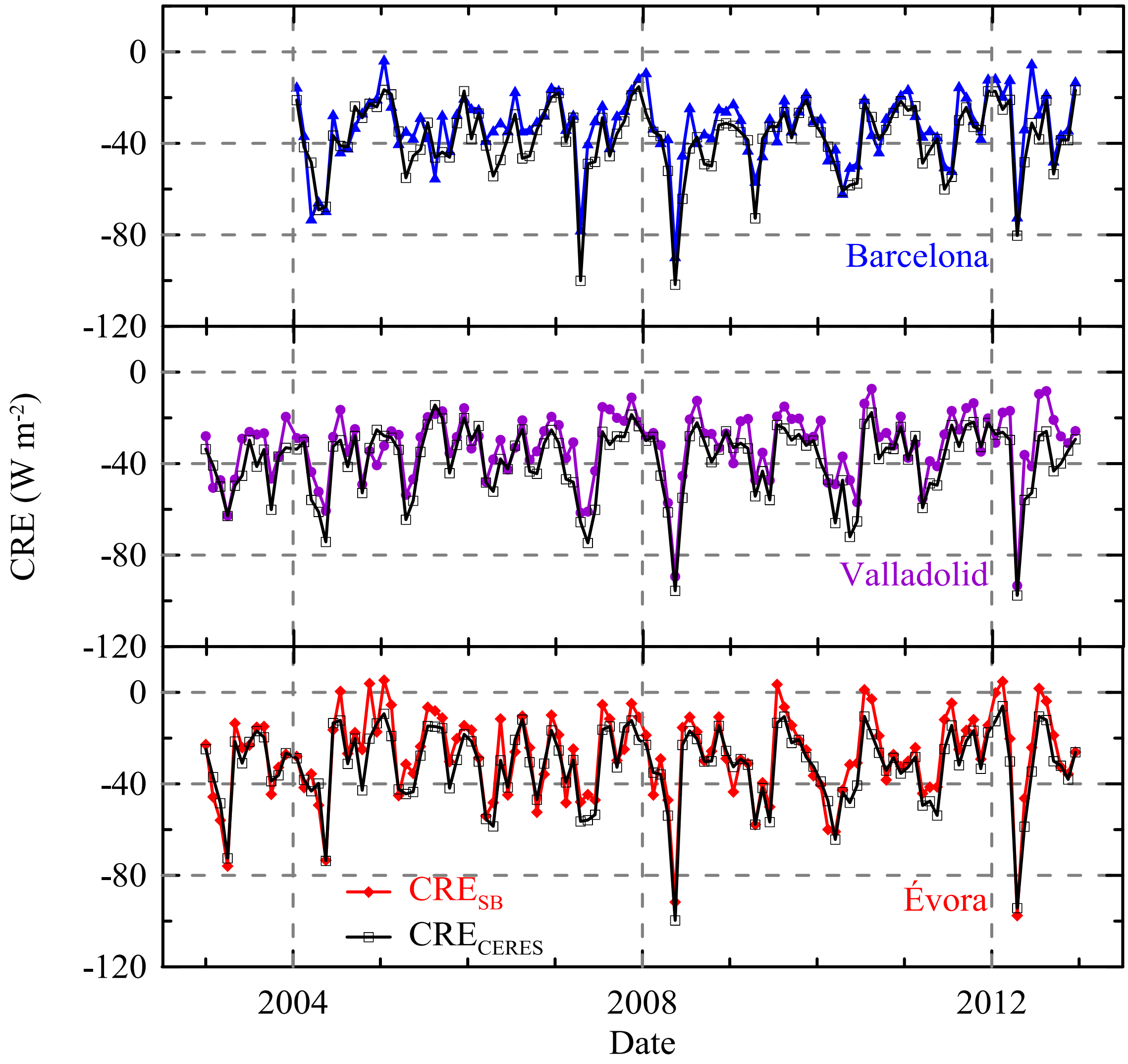

Figure 5. Monthly evolution of cloud radiative effect (CRE) using the method presented in this article (CRE_{SB}, solid symbols) and the estimations given by CERES (Clouds and the Earth's Radiant Energy System)-EBAF (Energy Balanced And Filled)-Surface (CRE_{CERES}, open squares).

Figure 6

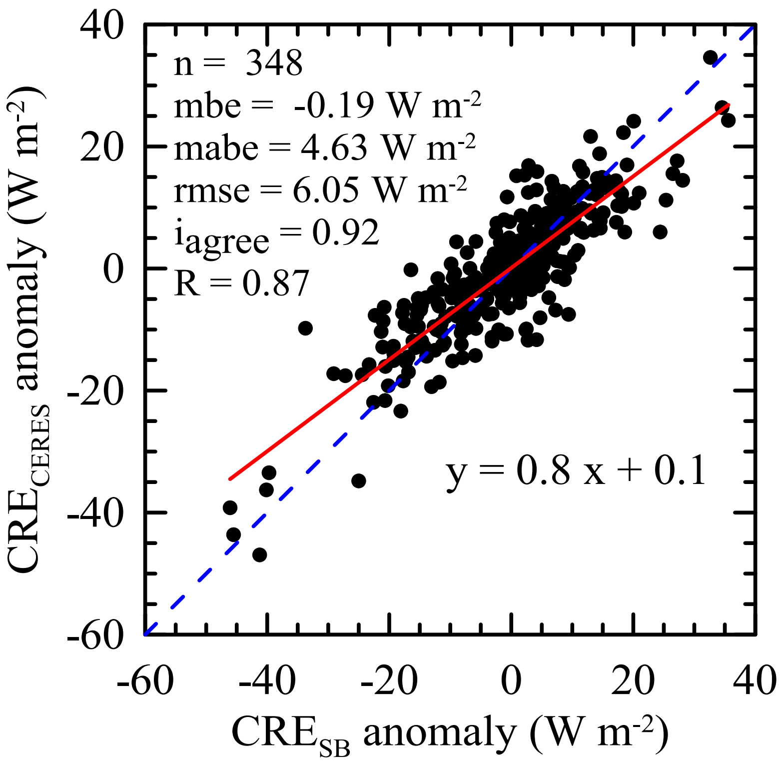

Figure 6. Scatter plot of cloud radiative effect monthly anomalies by the estimations given by CERES (Clouds and the Earth's Radiant Energy System)-EBAF (Energy Balanced And Filled)-Surface (CRE_{CERES}) and by the method presented in this article (CRE_{SB}). The solid line points out the linear fit, and the dashed line is the 1:1 line. Legend: n (number of data), mbe (mean bias error), mabe (mean absolute bias error), rmse (root mean square error), i_{agree} (index of agreement) [*Willmott*, 1982], and R (correlation coefficient).